Simulation of Mullins effect and permanent set in filled elastomers using multiplicative decomposition

S. M. Govindarajan & J. A. Hurtado
ABAQUS, Inc., Rising Sun Mills, 166 Valley St, Providence, RI 02909 USA

W. V. Mars
Cooper Tire & Rubber Co., 701 Lima Avenue, Findlay OH 45840, USA

ABSTRACT: Stress softening, also known as Mullins effect, can be observed in filled-elastomers, after subjecting a virgin specimen to an initial load. There is often an associated permanent set, or plastic deformation, observed upon removal of the load. Both Mullins effect and permanent set can be usefully idealized as irreversible. In this paper, we present a theory based on a multiplicative split of the deformation gradient, into elastic and plastic components, that may be used to model both permanent set and Mullins effect. Stress softening is modeled using a modified version of Ogden and Roxbourgh's (1999) theory. Plasticity is modeled in the context of finite strains using a Mises yield condition, and an associated flow rule. This theory has been implemented into the commercial finite element software Abaqus. The results of FE simulation of loading / unloading of a test specimen in simple modes, such as uniaxial tension, compare well with the experimental data for an EPDM polymer material. The theory is also used to simulate the combined axial / torsional deformation of an axisymmetric rubber ring. The results of the simulation including Mullins effect and permanent set compare well with the experimental observations and represent a significant improvement over the results obtained when permanent set is neglected in the simulation.

1 INTRODUCTION

This work is concerned with the modeling of stress-softening, also known as Mullins effect (Mullins 1969), and the associated permanent set, or inelastic effects, which can be observed when a filled-elastomer is subject to loading-unloading cycles (Mars and Fatemi, 2004a). Both effects can be observed in Figure 1 where the typical uniaxial response of a filled-elastomer is shown. After several cycles between zero stress and a fixed-strain-level have been applied to the specimen, it shows a stable stress-strain response accompanied by dissipation of energy through a hysteresis loop. Further softening and accumulation of permanent set occur when the specimen is strained to a higher strain level.

A model for the stress-softening effect has been available for several years (Bose et al 2003) in the commercial finite element software Abaqus. The model is based on the pseudo-elastic theory of Ogden and Roxburgh (1999). Mars (2004) used this model to simulate the combined effects of axial and torsional deformation on stress softening, ignoring the effects of permanent set. Dorfmann and Ogden (2004) formulated a pseudo-elastic strain energy function aimed at capturing both permanent set and stress-softening. Their model depends not only on

the deformation gradient, but also on two additional state variables.
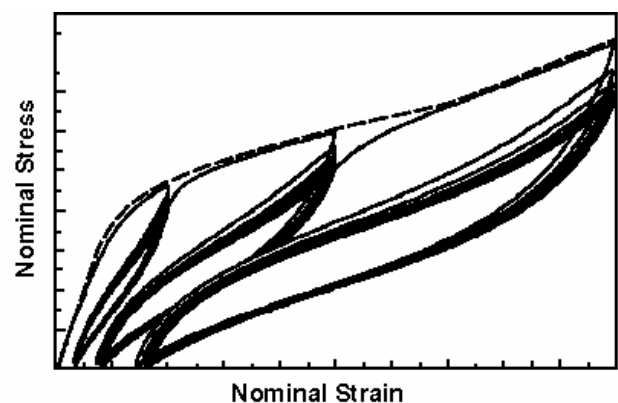

Figure 1. Typical response of filled-elastomers under cyclic loading conditions

In our work, we use Mises plasticity with an associated flow rule to model permanent set in the context of finite strain elasticity using a multiplicative decomposition (Lee 1969). In addition, stress-softening effects, modeled through a modified Ogden-Roxburgh model (1999), are combined with the effects of permanent set.

The paper is organized as follows. First a brief description of the plasticity constitutive equations

based on multiplicative decomposition is provided. Next, a discussion on calibration of the model, and on splitting experimental data into plastic, hyperelastic, and damage contributions is outlined. Then validation of the model in simple deformation modes is presented. Finally, the results of simulation of combined axial and torsional loading of a rubber component is compared with that of experimental data.

Standard notations are used throughout the paper. Boldface symbols are used to denote tensors, with their orders indicated by the context. If $\mathbf{A}$ and $\mathbf{B}$ are second-order tensors, then the following product is used in the text: $(\mathbf{A} \cdot \mathbf{B})_{ij} = A_{ik}B_{kj}$.

2 FORMULATION

2.1 *Multiplicative decomposition*

In our formulation, both hyperelasticity and plasticity are assumed to be isotropic. In addition, plasticity is assumed to be isochoric. This assumption is consistent with observations of volumetric constitutive behavior of filled rubber reported by Mars (2004). The isotropic work hardening function is a nonlinear function of a scalar state variable, namely, the equivalent plastic strain $\bar{\varepsilon}^{p}$. The hardening function characterizes plastic dissipation in the material.

The starting point for our formulation is the multiplicative decomposition of the deformation gradient $\mathbf{F}$ into elastic and plastic parts (Lee 1969):

$$\mathbf{F} = \mathbf{F}^{e} \cdot \mathbf{F}^{p} , \tag{1}$$

where $\mathbf{F}^{p}$ is the fictitious intermediate configuration. After some straight-forward algebra the rate form of plastic deformation gradient may be written for isotropic materials (Dafalias 1984) as:

$$\dot{\mathbf{F}}^{p} = \mathbf{F}^{e^{-1}} \cdot \mathbf{D}^{p} \cdot \mathbf{F}^{e} \cdot \mathbf{F}^{p} , \tag{2}$$

where the plastic part $\mathbf{D}^{p}$ of the deformation rate tensor is given by the associated flow rule

$$\mathbf{D}^{p} = \frac{3\dot{\bar{\varepsilon}}^{p}}{2q}\bar{\boldsymbol{\tau}} \tag{3}$$

of the von Mises yield condition

$$q - \tau^{y}(\bar{\varepsilon}^{p}) = 0 . \tag{4}$$

In the above $\bar{\boldsymbol{\tau}}$ is the deviatoric part of the Kirchoff stress tensor $\boldsymbol{\tau}$; q is the effective Kirchoff stress defined as $q = \sqrt{\frac{3}{2}\bar{\boldsymbol{\tau}} : \bar{\boldsymbol{\tau}}}$; and τ^{y} is the nonlinear work hardening function, which depends on the equivalent plastic strain $\bar{\varepsilon}^{p}$.

The stress response is characterized through the hyperelastic strain energy potential W and is written as:

$$\boldsymbol{\tau} = \mathbf{F}^{e} \cdot 2\frac{\partial W(\mathbf{C}^{e})}{\partial \mathbf{C}^{e}} \cdot \mathbf{F}^{e^{T}} , \tag{5}$$

where $\mathbf{C}^{e} = \mathbf{F}^{e^{T}} \cdot \mathbf{F}^{e}$ is the right Cauchy-Green tensor.

2.2 *Mullins effect*

As shown in Figure 1, filled-elastomers exhibit both permanent set and stress-softening when a specimen is subject to cyclic loading. The stress softening effect (i.e. Mullins effect) is included in our formulation by incorporating a damage term in the strain energy potential in Equation 5 as follows:

$$W = W(\mathbf{C}^{e}, \eta) \tag{6}$$

where η is a scalar damage variable. Abaqus uses a modified Ogden-Roxburgh (1999) model to simulate stress-softening. The evolution of the scalar damage variable is written as

$$\eta = 1 - \frac{1}{r}\mathrm{erf}\left(\frac{\bar{W}^{\max} - \bar{W}^{\text{primary}}}{m + \beta\bar{W}^{\max}}\right) \tag{7}$$

In the above $\bar{W}^{\text{primary}}$ is the deviatoric part of strain energy in the primary loading path, $\bar{W}^{\max}$ is the maximum value of $\bar{W}^{\text{primary}}$ at the material point, r, m and β are material parameters, and $\mathrm{erf}()$ is the error function.

It should be mentioned that our model does not account for time and rate-effects, viscoelasticity or hysteresis effects.

2.3 *Solution update*

In the incremental development of nonlinear finite element solution, such as in Abaqus, the global equilibrium equations are solved using Newton's method. This implies that the state of the material must be updated at each integration point of the finite element mesh through an appropriate stress update procedure, and the exact linearization modulus must be computed in order to achieve quadratic-convergence of the global equilibrium equations.

The stress update procedure involves solving Equations 1-7 for a given total deformation $\mathbf{F}$ and the state of the material $\left(\mathbf{F}_{t}^{e}, \mathbf{F}_{t}^{p}, \bar{\varepsilon}_{t}^{p}, \bar{W}^{\max}\right)$ at the beginning of the current increment. This system of equations is solved using standard techniques outlined in Weber and Anand (1990) and Simo (1992). The algorithm implemented in Abaqus is first-order accurate and unconditionally stable. As mentioned earlier, the exact linearization modulus is computed for the stress update procedure.

3 CALIBRATION

As discussed in the previous section, our formulation needs the following characterization of filled elastomers, in order to carry out a finite element simulation: a hyperelastic response, a representation of

Mullins effect through a damage variable, and plasticity to model permanent set. These characterizations correspond to three different keywords in the definition of a material in Abaqus, namely, *HYPERELASTIC, *MULLINS EFFECT and *PLASTIC. In order to extract this information from Figure 1 we proceed as follows.

First the data in Figure 1 is divided into three tables of data corresponding to primary loading curve (shown in dashed line), unloading / reloading data and permanent set data. We assume that for a small non-zero stress there is no permanent set, which corresponds to the initial yield stress.

The curve of stress versus permanent strain defines the hardening function for the plasticity model. Using the table of permanent set data and the 1-d representation of the multiplicative decomposition, $\lambda = \lambda^e \lambda^p$, the primary loading response and the unloading response are computed in the unstressed intermediate configuration, which can be used directly as input to the program. Abaqus then automatically fits the model parameters associated with any of the available strain energy functions, as well as the constants r, m and β in the equation for the damage variable. The same calibration technique is applied to equibiaxial test data as well.

4 VALIDATION

Uniaxial test data for an EPDM compound is shown in dotted line (without markers) in Figure 2. After stretching the uniaxial specimen to 10% nominal strain, it was subject to 20 cycles between this strain and zero stress. Subsequently the strain levels were increased to 30% and 100% nominal strain. Clearly the material shows stress-softening while unloading, permanent set, and hysteretic dissipation of energy.

As described in the previous section, the plasticity hardening function was computed first. Then the primary loading response and the unloading response were computed in the intermediate configuration. Calibration of Mullins effect parameters was done using only the unloading data of the stable cycle. In our validation studies, the hyperelastic response was based on the first-invariant strain energy function of Marlow (2003), which is available in the finite element software Abaqus.

In the finite element simulation, a single element was subject to uniaxial loading to reach 10% nominal strain and then it was unloaded to zero stress level. Then the process was repeated for 30% and 100% strain levels. The finite strain elasto-plasticity model captures all three phases, namely, loading, unloading and permanent set very well.

Since we have ignored time and rate effects, as described earlier, any reloading after unloading does not show hysteresis effects, thus the reloading and the unloading paths coincide.
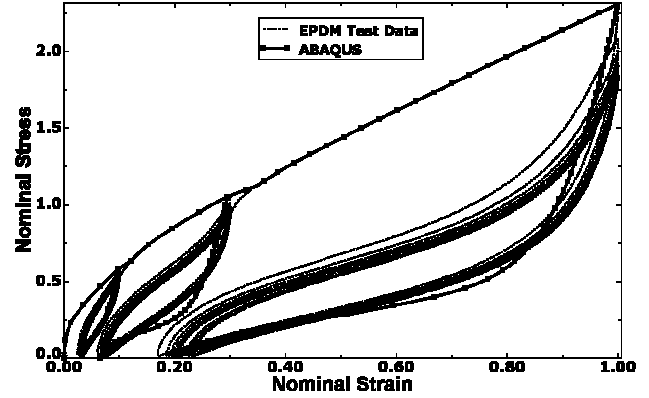

Figure 2. Abaqus simulation (solid line with markers) against EPDM polymer test data (dashed line without markers)

5 COMBINED AXIAL TORSIONAL LOADING

5.1 Specimen and Material Properties

Mars (2004, 2004b) has analyzed a thin-walled axisymmetric specimen subject to combined axial and torsional loading. The multi-axial stress states achieved in this specimen are typical of those that arise in applications such as rolling tires. In his analysis, Mars (2004) considered Mullins effect, but neglected permanent set. Here we show the results of simulation including permanent set.
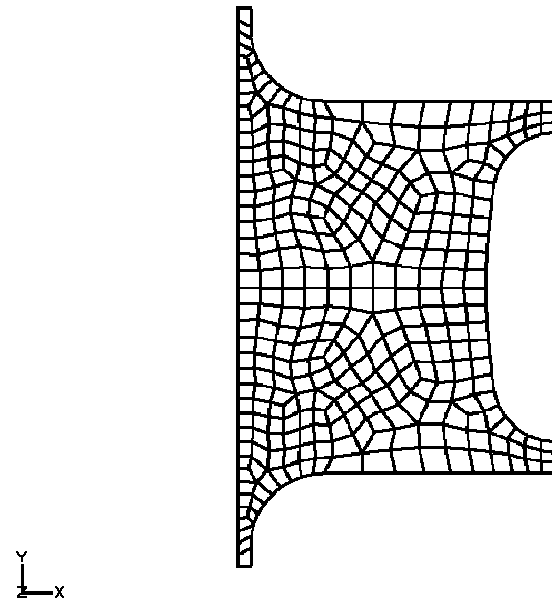

Figure 3. Finite element mesh of the axisymmetric specimen

The finite element mesh is shown in Figure 3. We have used the CGAX4H element of Abaqus for our simulations. This element allows modeling of twisting deformations that exhibit axisymmetry about the Y axis, and of incompressibility through a mixed-displacement-pressure formulation. All the nodes at

the bottom are constrained in the vertical direction, while they are free to twist and move radially as well. Axial displacement and rotation (twist) are applied at the top line of nodes.

Following Mars (2004), we use a 4th order reduced polynomial strain energy function to represent the hyperelastic response. The material properties for this model were calibrated based on pure axial and pure shear response of the aforementioned specimen and are listed in the following equation.

$$c_{10} = 146.74 \text{ MPa}, \; c_{20} = 6.5252 \text{ MPa},$$
$$c_{30} = 0, \; c_{40} = -0.028648 \text{ MPa} \tag{8}$$

Likewise the parameters in Equation 7 used to model Mullins effect are:

$$r = 3, \; m = 56.282 \text{ MPa}, \; \beta = 0.1 \tag{9}$$

Plasticity is characterized by a linear hardening function $\tau^y = \tau_0^y + H\bar{\varepsilon}^p$ with

$$\tau_0^y = 29.6679 \text{ MPa}, \; H = 8168.04 \text{ MPa}. \tag{10}$$

5.2 Results

The results of finite element simulation with and without permanent set are compared with the experimental results for two different loading paths. In Figure 4, paths H and I are shown, which correspond to the out-of-phase axial and torsional loads. In both cases, displacement and rotation boundary conditions are applied to the top lines of nodes for axial and torsion loading respectively.
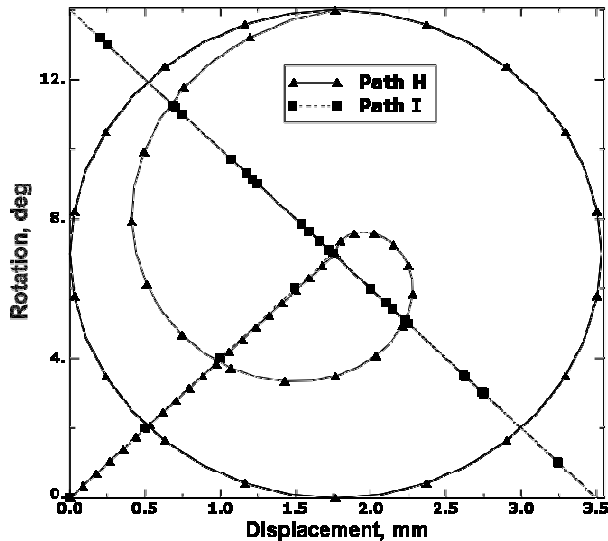
Figure 4. Combined axial/torsional loading paths H and I

In the following figures, axial load is computed as the sum of the axial reaction forces in the top line of nodes. Similarly, torque is computed as the sum of the reaction moments about the vertical axis in the top line of nodes. The experimental data is shown by long dashed-lines with open markers, while finite element simulations with and without permanent set are shown by solid lines (labeled Fe.Fp) and short dashed-lines (labeled Fe) respectively.

Figure 5 shows axial load against axial displacement for the final circular portion of Path H. The torsion response during the same test is shown in Figure 6. In this loading path, axial and torsional actuations are 90° out of phase. The simulation results including permanent set show good agreement with the experiment. In particular, both the elastic behavior and the permanent set have been accurately rendered, for both axial and torsion responses.
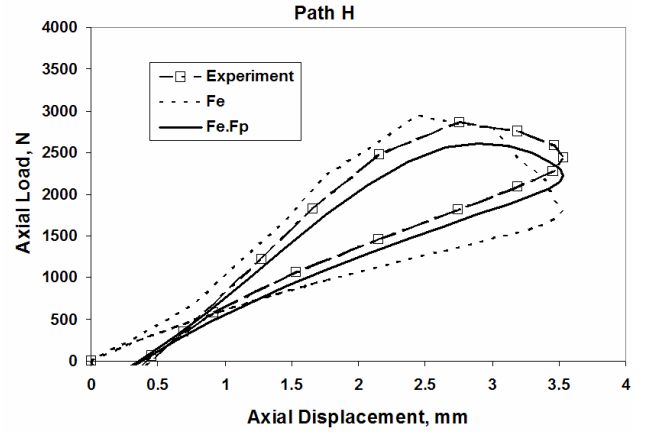
Figure 5. Axial response for path H (combined axial/torsional loading 90° out of phase)
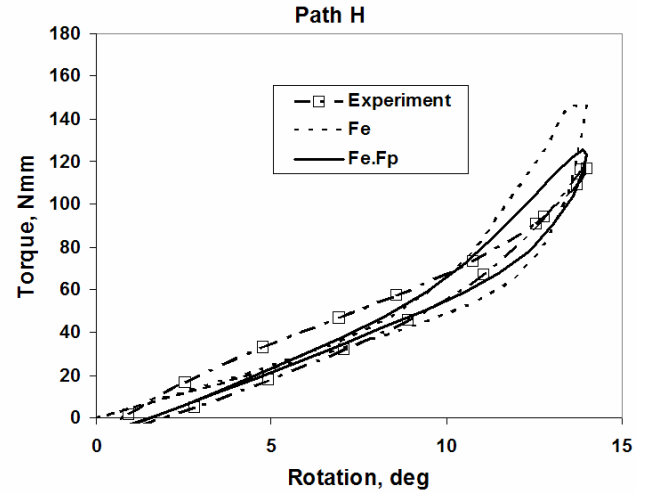
Figure 6. Torsional response for path H (combined axial/torsional loading 90° out of phase)

Figures 7 and 8 show, respectively, the axial and torsion responses for Path I. In this loading path, axial and torsional actuations are 180° out of phase. In this case, it can be clearly seen how including permanent set improves agreement between experiment and prediction. Note particularly the axial response: without permanent set, a very soft behavior is predicted. Prediction of the torsional response is also slightly improved. By including permanent set, both axial and torsional responses can be accurately modeled.
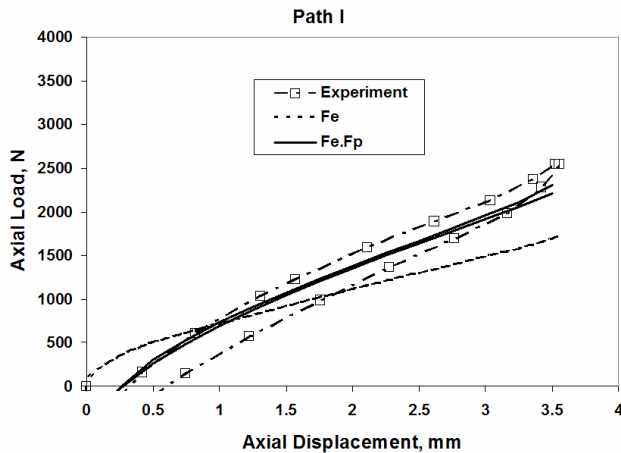
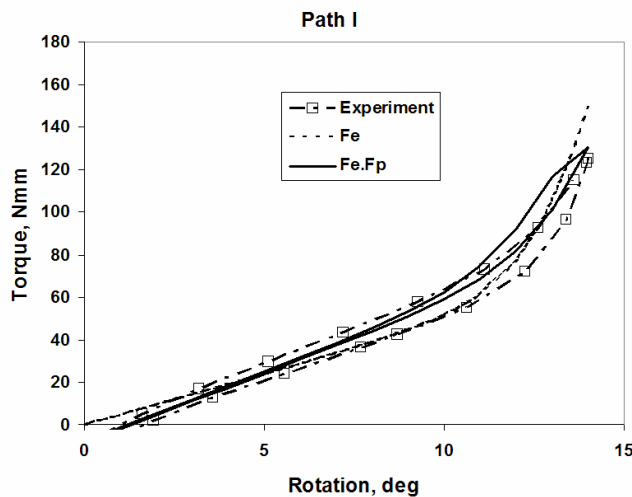Figure 7. Axial response for path I (combined axial/torsional loading 180° out of phase)

Figure 8. Torsional response for path I (combined axial/torsional loading 180°out of phase)

6 CONCLUSION

We have formulated a rate-independent theory that captures the effects of permanent set and stress softening for a class of filled elastomers. The model has been implemented in the commercial finite element software Abaqus. This theory is based on the principle of multiplicative decomposition of the deformation gradient and hence is valid for finite elastic strains. Our formulation avoids the oscillatory stress solution generated by finite elastic shear strains when the Jaumann rate is employed, as shown by Nagtegaal and de Jong (1982).

The constitutive model has been validated by comparing finite element results with experimental results in a simple deformation mode for an EPDM polymer. We were also able to obtain excellent

agreement in results for a filled rubber component when subject to combined axial / torsional loading.

In summary, the ability to calibrate material parameters for filled elastomers, and the ability to model permanent set and Mullins effect is a powerful simulation tool.

ACKNOWLEDGEMENTS

REFERENCES

Bose, K. Hurtado, J. Snyman, M. Mars, W.V. & Chen, J.Q. 2003. Modeling of stress softening in filled elastomers, *Proceedings of the 3rd ECCMR*, Busfield, J.J.C. & Muhr, A.H. (eds), Swets and Zeitlinger, Netherlands 223-230.

Dafalias, Y.F. 1984. The plastic spin. *Journal of Applied Mechanics* 52: 865.

Dorfmann, A. & Ogden, R.W. 2004. A constitutive model for the Mulins effect with permanent set in particle-reinforced rubber. *International Journal for Solids and Structures* 41: 1855-1878.

Lee, E.H. 1969. Elastic-plastic deformation at finite strains. *Journal of Applied Mechanics* 36:1-6.

Marlow, R.S. 2003. A general first-invariant hyperelastic constitutive model. *Proceedings of the 3rd ECCMR*. Busfield, J.J.C. & Muhr, A.H. (eds), Swets and Zeitlinger, Netherlands 157-160.

Mars, W.V. 2004. Evaluation of a pseudo-elastic model for the Mullins effect. *Tire Science and Technology* 32: 120-145.

Mars, W. V. & Fatemi, A. 2004a. Observations of the constitutive response and characterization of filled natural rubber under monotonic and cyclic multiaxial stress states, *Journal of Engineering Materials and Technology* 126: 19-28.

Mars, W. V. & Fatemi, A. 2004b. A novel specimen for investigating mechanical behavior of elastomers under multiaxial loading conditions, *Experimental Mechanics* 44: 136-146.

Mullins, L. 1969. Softening of rubber by deformation. *Rubber Chemistry and Technology* 42: 339-362.

Nagtegaal, J.C. & de Jong, J.E. 1982. Some aspects of nonisotropic work hardening in finite strain plasticity. *Plasticity of metals at finite strain: theory, experiment and computation*. Lee, E.H & Mallet, R.L. (eds), Stanford University Press: 65.

Ogden, R.W. & Roxburgh, D.G. 1999. A pseudo-elastic model for the Mullins effect in filled rubber. *Proceedings of the Royal Society of London*. 455(A): 2861-2877.

Simo, J.C. 1992. Algorithms for static and dynamic multiplicative plasticity that preserve the classical return mapping schemes of the infinitesimal theory. *Computer Methods in Applied Mechanics and Engineering* 99: 61-112.

Weber, G. & Anand, L. 1990. Finite deformation constitutive equations and a time integration procedure for isotropic hyperelsatic-viscoplastic solids. *Computer Methods in Applied Mechanics and Engineering* 79: 173-202.